

Probing the limit of one-dimensional heat transfer under extreme bending strain

Victor Lee,^{1,2} Renkun Chen,³ and Chih-Wei Chang^{1,*}

¹*Center for Condensed Matter Sciences, National Taiwan University, Taipei 10617, Taiwan*

²*Department of Physics, National Taiwan University, Taipei 10617, Taiwan*

³*Department of Mechanical and Aerospace Engineering, University of California at San Diego, La Jolla, California 92093, USA*

(Received 4 May 2012; published 8 January 2013)

Theoretically, when a one-dimensional (1D) ballistic thermal conductor is mechanically bent beyond its elastic limit, nonlinear structural buckling will develop and reduce the transmission of phonons. However, because of limited mechanical strengths and short phonon mean free paths of most materials, no experimental works are capable of testing this fundamental limit of heat transfer so far. Here, we utilize the superior mechanical strength and the high thermal conductivity of single-wall carbon nanotubes (SWCNTs) to investigate the heat transfer phenomena at a previously inaccessible experimental regime. Surprisingly, even when the SWCNTs are bent far beyond their critical angles and curvatures, their thermal conductivities remain intact under cyclic bending. Moreover, the observed robustness of heat transfer is found to be independent of structural kinks, defects, dislocations, bending angles, or curvatures. Our results demonstrate that SWCNTs are exceptional 1D thermal conductors capable of sustaining high transmission of phonons under extreme bending strain.

DOI: [10.1103/PhysRevB.87.035406](https://doi.org/10.1103/PhysRevB.87.035406)

PACS number(s): 66.70.Df, 61.48.De, 65.80.—g

The particle picture of phonon transport in a solid is similar to the energy transfer of gas molecules confined in a box with one end of the box being hotter than the other end.¹ Different phonon scattering processes in a solid are thus similar to different kinds of collisions of gas molecules in the box that give rise to finite thermal conductivity (κ). Therefore, the phonon mean free path (l_{mfp}) of a solid can be viewed as the averaged distance of a gas molecule (in analogy to a phonon) undergoing two successive collisions. Various phonon scattering mechanisms are known to reduce κ , including phonon-phonon scatterings, impurity scatterings, boundary scatterings, and others. Applying the established knowledge to understand phonon transport under bending strain is particularly intriguing, especially for one-dimensional (1D) systems in which heat transfer phenomena are predicted to be singular.²

When a 1D material like a single-wall carbon nanotube (SWCNT) is mechanically bent beyond its elastic limit, the strain energy will be released via the formation of a structural kink.^{3,4} When going further beyond the critical strain, the SWCNT may develop different forms of kinks, as shown in Fig. 1.³ In one case, the cross section of the kink experiences progressive ovalization with increasing bending angle.⁵ In another case, multiple kinks may develop in a long SWCNT under large bending angles.⁶ Lastly, the kink may widen and connect to adjacent structural buckles to form complex geometries.⁷ Although the formation of the postbuckling structures depends on the details of sample diameters, lengths, and chiralities,⁶ based on the simple picture of phonon transport mentioned above, it is anticipated that the structural kinks could be efficient phonon scatterers for reducing κ . Moreover, for a ballistic thermal conductor (i.e., sample length (L) $\sim l_{\text{mfp}}$), the reduction of κ is expected to be more pronounced than for a diffusive thermal conductor (i.e., $L \gg l_{\text{mfp}}$).

Many detailed theoretical calculations have supported the simple picture.^{8–11} Various molecular dynamics simulations on SWCNTs under strain have suggested that the phonon scattering rate increases significantly when the structure

buckles.^{8,9} Although the formation of structural kinks only affects the spectrum of high-frequency phonons (>50 THz), and the low-frequency phonons dominating the heat transfer of a SWCNT remain unaffected,^{8,11} the local kink formed at the bending angle 30° is calculated to contribute an interface conductivity of approximately $50 \text{ GW/m}^2\text{K}$,⁸ and it becomes five times resistive when the bending angle increases to 60° ,¹¹ comparable to that of hetero-junctions or point defects.¹¹ In fact, a 10% reduction of κ is predicted when column (Euler) buckling occurs in a SWCNT.⁸ Continuously increasing the strain will monotonically reduce the κ to 20 ~ 60% of the unstrained value when the compressive strain exceeds 5% and a local kink is created.^{8,10}

Experimentally testing the limit of 1D heat transfer under bending strain is important for fundamental understandings of 1D phonon scattering mechanisms and for potential applications in developing thermal devices, such as thermal switches and thermal interface materials. Interestingly, previous experimental work on multiwall carbon nanotubes and multiwall boron-nitride nanotubes showed unexpected robustness of κ 's, to which no observable changes have been resolved for bending angles larger than 130° .¹² Moreover, the phonon propagation seems to be unaffected by the structural ripples formed at the deformed region, indicating that phonon transport in nanotubes is appreciably different from the conventional thermal conductors. The bent nanotubes thus represent an emergent class of materials to test the fundamental limit of heat transfer. Unfortunately, given the complex layer-layer interactions in a multiwall nanotube, direct comparisons between theories and experiments are difficult. Additionally, the multiwall nanotubes investigated in the previous experiment exhibit $L/l_{\text{mfp}} > 25$, rendering the bending effect on phonon transmission, if present, difficult to observe because of their diffusive phonon transport nature.¹² An ultimate experimental test of the 1D ballistic heat transfer phenomena would prompt for materials with sufficiently long l_{mfp} and an outstanding strain sustainability to reach the extreme condition.

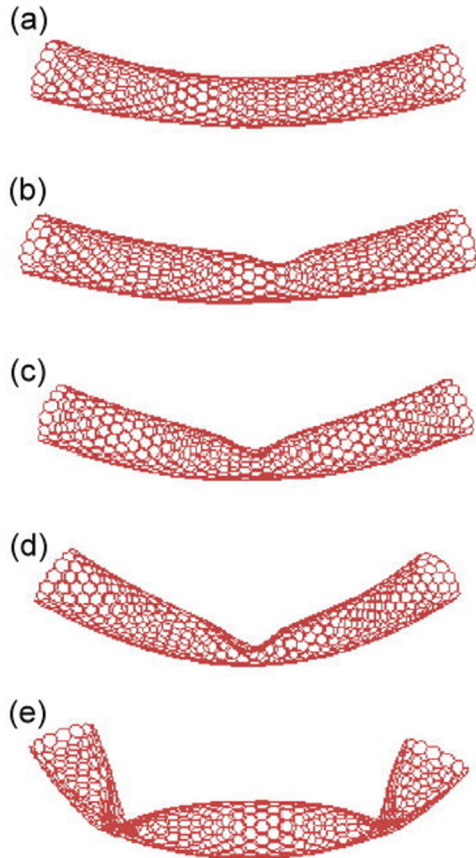


FIG. 1. (Color online) The morphologies of a (15,0) SWCNT under bending strain. (a) Before critical angle, (b) bending angle of 37° , (c) bending angle of 46° , (d) bending angle of 68° , (e) bending angle of 126° . The figures are redrawn from Ref. 3. Copyright permission granted.

SWCNTs are ideally suited 1D systems for this purpose because of their extraordinary mechanical strength (>100 GPa) and superior thermal conductivity (>2000 W/m-K at 300K).¹³ In particular, phonon transport in the cylindrical-structured nanotubes have been shown to exhibit many fascinating phenomena, including 1D phonon confinements,^{14,15} phonon waveguiding,¹² thermal rectification,¹⁶ violation of Fourier's law,¹⁷ and tunable thermal links.¹⁸ These features make investigating phonon transport of nanotubes particularly interesting. Importantly, SWCNTs exhibit very long l_{mfp} 's that will allow us to rigorously test the limit of heat transfer of a 1D ballistic thermal conductor under extreme bending strain.

Experimentally, high-quality SWCNTs were grown using chemical vapor deposition (CVD) methods.^{19–22} Solutions of 0.001 M FeCl_3 in water were used as catalysts. SWCNTs were synthesized in a quartz tube at 925°C under a flow of mixed Ar/ethanol gas at the rates of 150 and $400\text{ cm}^3/\text{min}$, respectively. The ethanol CVD method produced long, suspended SWCNTs across the slits of Si substrates. Individual SWCNTs were picked up by a custom-designed manipulator and placed on a microscale thermal conductivity test fixture.²³ As shown in Fig. 2, the test fixture consists of two integrated Pt film resistors supported by suspended SiN_x pads. The Pt film resistors serve as independent heaters and sensors for measuring the Joule heating power (P)

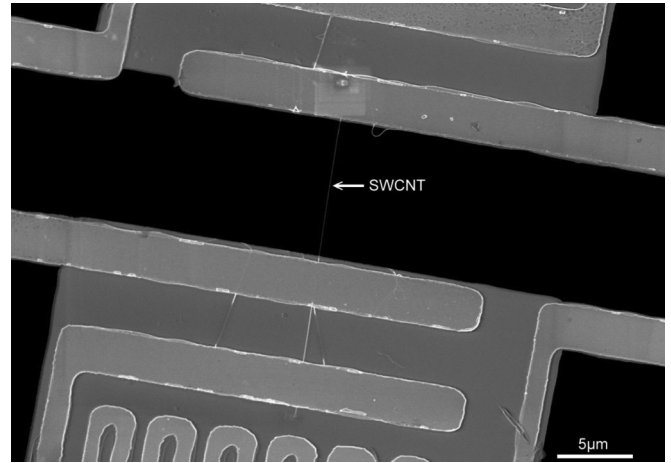


FIG. 2. A scanning electron microscopy (SEM) image of a microscale thermal conductivity test fixture with a SWCNT spanning the suspended heater/sensor pads.

and temperature variations (ΔT_h and ΔT_s). Under steady state, the thermal conductance (K) of the nanotube can be obtained using the relation

$$K = \frac{P}{\Delta T_h - \Delta T_s} \left(\frac{\Delta T_s}{\Delta T_h + \Delta T_s} \right). \quad (1)$$

In situ mechanical bending and thermal conductivity measurements were carried out using a piezo-driven manipulator inside a SEM. We found that pristine SWCNTs can bond rigidly to the heater/sensor pads during cyclic mechanical bending. Additionally, depositing Pt/C composites or varying the anchored lengths of the SWCNT had negligible effects on total K . We concluded that thermal contact resistance was minimal; thus, no extra electron-beam-induced deposition was made during the experiment to avoid unattended contaminations. We had carefully removed the background contributions due to near-field radiation heat transfer. After the measurement, the samples were transferred into a transmission electron microscope (TEM) for unraveling the diameters (usually in the range of $1 \sim 2$ nm) of the investigated SWCNT. We have used conventional thickness (0.34 nm) to estimate the cross-sectional area of SWCNTs. The l_{mfp} of each sample was first estimated using the conventional 1D kinetic theory, namely, $\kappa = C_{\text{bulk}} v_{\text{bulk}} l_k$, where C_{bulk} is the volumetric specific heat (8×10^5 J/K-m³), v_{bulk} is the averaged sound velocity (15 km/s), and l_k is the phonon mean free path determined by the kinetic theory. We have noted that the kinetic theory overestimates the specific heat contributions from optical phonons and ignores the realistic frequency dispersions of the material. As a result, it underestimates l_{mfp} , and the l_k 's should be corrected in accord with the results on length dependence of κ (see Supplementary Material²⁴). We find that the l_k should be multiplied by a factor of 5.7 to be consistent with earlier theoretical and experimental results on the l_{mfp} .^{25,26} The l_{mfp} 's of the investigated SWCNTs are in the range of $533 \sim 912$ nm.

The upper images of Fig. 3 display four different SWCNTs undergoing cyclic bending. The κ 's of SWCNTs are normalized to their initial values of 1341, 1237, 2007, and

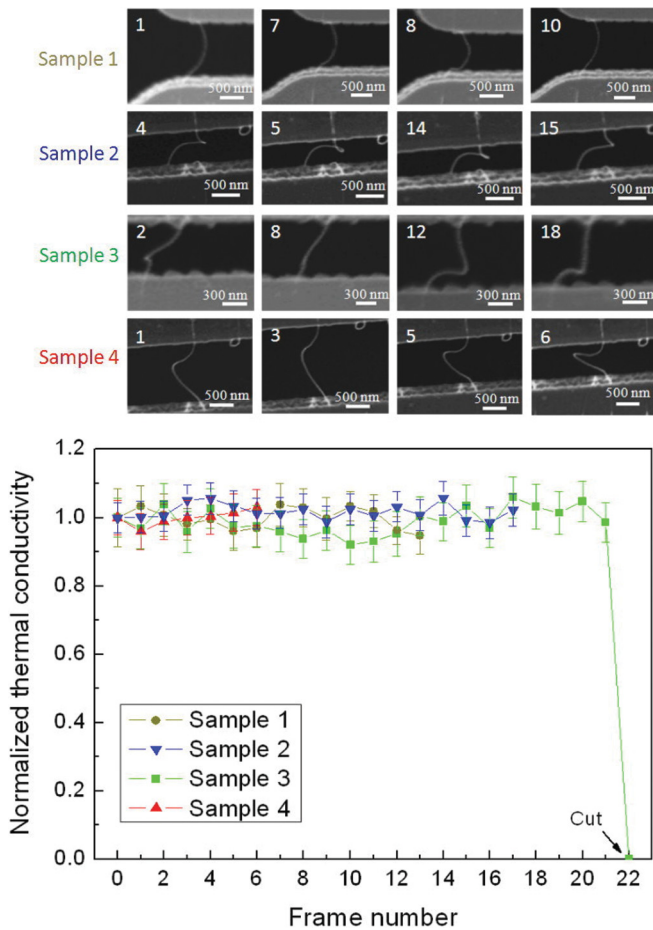


FIG. 3. (Color online) Upper images: Representative SEM images of Samples 1 to 4 undergoing cycles of bending. The number of each image denotes the frame number in the lower panel. Lower panel: The corresponding κ (normalized to their initial values) measured during the bending. The last data point of Sample 3 shows κ reducing to zero when the sample was cut using an electron beam. The κ 's of SWCNTs are normalized to their initial values of 1341, 1237, 2007, and 1172 W/m-K, respectively. The SWCNTs are near the ballistic thermal transport regimes, as their L/l_{mfp} 's are found to be less than 2.8, 2.7, 1.6, and 5.1 for Samples 1 to 4, respectively.

1172 W/m-K, respectively. Under external stress, SWCNTs are compliant and can be bent into different shapes. We notice that for Sample 1 and Sample 2, the shapes always buckle at the same location for different cycles of bending (see frames 1 and 8 for Sample 1 and frames 5 and 14 for Sample 2). On the other hand, the bends do not repeat themselves for Sample 3 (see frames 2, 8, 12, and 18) for four cycles of bending (only one cycle of bending was conducted in Sample 4). Because the presence of defects or dislocations will help the SWCNTs relax their strain energy easily at the structurally imperfect regions,^{27–29} the observation indicates the presence of permanent defects or dislocations in Sample 1 and Sample 2, whereas they are absent in Sample 3. Since the defects or dislocations are phonon scatters, their presence/absence will also affect phonon transport of SWCNTs. As expected, κ 's of Samples 1 and 2 are smaller than that of Sample 3.

Remarkably, despite the presence/absence of defects or dislocations and the severe structural deformation shown in

Fig. 3, all SWCNT κ 's stay at the initial values within the experimental error bars ($\sim 10\%$). As shown in the lower panel of Fig. 3, no correlation between κ and structural geometries is observed for any of the four samples. The results show that cyclic bending does not affect the thermal transport properties of SWCNTs. Surprisingly, bending angles do not affect the κ 's, either. In fact, reductions of κ only occurred when we employed a focused electron beam to permanently cut the SWCNT, as shown in the last data point of Fig. 3.

To analyze the unusual robustness of κ quantitatively, we note that the formation of kinks in a bent SWCNT depends on the critical angle (θ_c) and the critical radius of curvature (R_c).⁴ For the investigated SWCNTs with diameters ~ 2 nm, calculations have suggested $\theta_c = 30^\circ$ and $R_c = 50$ nm.⁶ Notably, the calculations have not considered the effect of defects. In fact, molecular dynamics simulations have shown that a single defect can reduce the buckling load and the critical strain of a SWCNT by more than 30%.^{27–29} Thus, it is expected that kinks can be easily created at $\theta_c < 30^\circ$ and $R_c > 50$ nm for a defective SWCNT.

At the extremes of bending strain shown in Fig. 4, the bending angles are 70° , 124° , 145° , and 162° for Samples 1 to 4, respectively. The minimum radii of curvature can be obtained from the projective and tilted SEM images before and after the bending. Figure 4 displays the SEM and corresponding reconstructed 3D images when the SWCNTs are extremely deformed. The minimum radii of curvature reach 190, 56, 45, and 22 nm for Samples 1 to 4, respectively. Due to the presence of defects and the large bending angles in Samples 1 and 2, it is likely that kinks have been created in Fig. 4. For Samples 3 and 4, both the bending angles and the radii of curvature have gone far beyond θ_c and R_c . Clearly, kinks with severely deformed structures similar to Fig. 1 must have been created in Fig. 4. Remarkably, still no reduction of κ is observed. We have estimated the l_{mfp} 's to be 609, 562, 912, and 533 nm for Samples 1 to 4, respectively. Comparing to the respective sample lengths (L), L/l_{mfp} is found to be less than 2.8, 2.7, 1.6, and 5.1 for Samples 1 to 4, respectively. Undoubtedly, all the investigated SWCNTs are near the ballistic thermal transport regime.

The robustness of κ tested at the severely buckled conditions clearly refines the limit of 1D heat transfer anticipated intuitively. Our experimental results also disagree with earlier theoretical predictions of a bent SWCNT.^{8–11} The interactions between phonons and kinks are much weaker than expected, which indicates that phonons with very long wavelengths are responsible for heat conduction in a SWCNT. The experimental results also indicate that the equivalent interfacial thermal resistance of the kink exhibits a much shorter effective length than suggested.⁸ Furthermore, the contributions of high-frequency phonons to SWCNT κ 's could be overestimated.^{8–11}

Alternatively, some molecular dynamics simulations have suggested that reductions of SWCNT κ 's can happen before the formation of local kinks.^{8,10} For this alternative case, the geometrical curvature effect and the strain effect on κ 's should be considered. It has been theoretically suggested that the geometrical curvature effect can enhance phonon back scatterings of high-frequency phonons, leading to 10 \sim 15% reduction in SWCNT κ 's when $l_{\text{mfp}}/R = 1 \sim 6.2$ (where R is the radius of curvature).^{8,10} In our experiment,

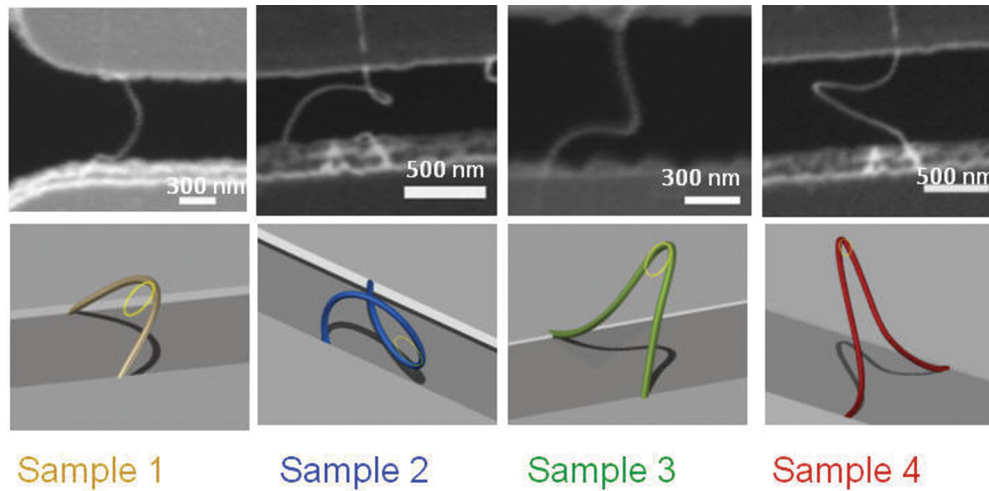


FIG. 4. (Color online) SEM images of Samples 1 to 4 under extreme bending strain (upper row) and the corresponding reconstructed three-dimensional (3D) images (lower row). The shadowed curves display the projective (SEM) images of SWCNTs, and the yellow circles denote the minimum radius of curvature of each sample. The bending angles are 70° , 124° , 145° , and 162° for Samples 1 to 4, respectively. The minimum radii of curvature are 190, 56, 45, and 22 nm for Samples 1 to 4, respectively.

the insensitivities of κ 's tested at $l_{\text{mfp}}/R = 3.2, 10.2, 20.3,$ and 24.2 for Samples 1 to 4, respectively, indicate much weaker phonon back scatterings than theoretically anticipated. For comparison, a 15% reduction in the κ of serpentine Si nanowires has been theoretically suggested when $l_{\text{mfp}}/R = 7.3$,³⁰ but the experimental observation instead displays a much pronounced effect (i.e., a 40% reduction in the κ when $l_{\text{mfp}}/R = 0.5$).³¹ Although the marked differences between the SWCNTs and the serpentine Si nanowires can be arguably attributed to the absence of boundary scatterings in SWCNTs, it remains unclear why the effect of tensile strain on the outer shell can be exactly compensated by the effect of compressive strain on the inner shell for an extremely bent SWCNT.⁹ Comparing with the previous work that multiwall nanotubes were tested below $l_{\text{mfp}}/R = 0.7$,¹² the severe conditions tested here ($l_{\text{mfp}}/R = 24.2$) in fact set a new limit of robustness of heat transfer in SWCNTs. Notably, although our experimental results disagree with some molecular dynamics simulations on a 50-nm-long SWCNT,^{8,10} they are consistent with simulations on a considerably longer (126-nm) SWCNT.³² Thus, the low-frequency phonons that lead to anomalous violations of Fourier's law in 1D systems could be overlooked in some

theoretical modeling. Future molecular dynamics simulations on SWCNTs of longer lengths and employing full quantum effects may help elucidate the puzzle.

In summary, we find that κ 's of SWCNTs exhibit unusual robustness against bending strain. The robustness of heat transfer has been experimentally tested far beyond the elastic limit of bending and is found to be independent of defects, dislocations, structural kinks, bent angles, or bent curvatures. The refined robustness limit of κ in severely deformed SWCNTs will pose more interesting questions regarding the foundations of heat transfer. The criteria of Fourier's law and the 1D heat transfer problem has been a theoretical puzzle for decades, but not until recently did it become experimentally accessible.^{17,33} The present experimental findings on SWCNTs may stimulate further explorations of the 1D thermal conductors in both experimental and theoretical aspects.

We thank Dr. Ming-Wen Chu for TEM characterizations and Mr. Tzu-Kan Hsiao for experimental assistance. This work was supported by the National Science Council of Taiwan (NSC98-2112-M-002-021-MY3) and Academia Sinica (AS-101-TP2-A01).

*cwchang137@ntu.edu.tw

¹C. Kittel, *Introduction to Solid State Physics* (Wiley, New York, 2004).

²A. Dhar, *Adv. Phys.* **57**, 457 (2008).

³X. Guo, A. Y. T. Leung, X. Q. He, H. Jiang, and Y. Huang, *Compos. Part B-Eng.* **39**, 202 (2008).

⁴H. Shima, *Materials* **5**, 47 (2012).

⁵A. Kutana and K. P. Giapis, *Phys. Rev. Lett.* **97**, 245501 (2006).

⁶G. X. Cao and X. Chen, *Phys. Rev. B* **73**, 155435 (2006).

⁷X. Yao, Q. Han, and H. Xin, *Comput. Mater. Sci.* **43**, 579 (2008).

⁸Z. P. Xu and M. J. Buehler, *Nanotechnology* **20**, 185701 (2009).

⁹X. Li, K. Maute, M. L. Dunn, and R. Yang, *Phys. Rev. B* **81**, 245318 (2010).

¹⁰Z. X. Huang, Z. Tang, J. Yu, and S. Y. Bai, *J. Appl. Phys.* **109**, 104316 (2011).

¹¹F. Nishimura, T. Shiga, S. Maruyama, K. Watanabe, and J. Shiomi, *Jpn. J. Appl. Phys.* **51**, 015102 (2012).

¹²C. W. Chang, D. Okawa, H. Garcia, A. Majumdar, and A. Zettl, *Phys. Rev. Lett.* **99**, 045901 (2007).

¹³A. A. Balandin, *Nat. Mater.* **10**, 569 (2011).

¹⁴J. Hone, M. Whitney, C. Piskoti, and A. Zettl, *Phys. Rev. B* **59**, R2514 (1999).

- ¹⁵J. Hone, B. Batlogg, Z. Benes, A. T. Johnson, and J. E. Fischer, *Science* **289**, 1730 (2000).
- ¹⁶C. W. Chang, D. Okawa, A. Majumdar, and A. Zettl, *Science* **314**, 1121 (2006).
- ¹⁷C. W. Chang, D. Okawa, H. Garcia, A. Majumdar, and A. Zettl, *Phys. Rev. Lett.* **101**, 075903 (2008).
- ¹⁸C. W. Chang, D. Okawa, H. Garcia, T. D. Yuzvinsky, A. Majumdar, and A. Zettl, *Appl. Phys. Lett.* **90**, 193114 (2007).
- ¹⁹M. Hofmann, D. Nezich, A. Reina, and J. Kong, *Nano Lett.* **8**, 4122 (2008).
- ²⁰B. H. Hong, J. Y. Lee, T. Beetz, Y. M. Zhu, P. Kim, and K. S. Kim, *J. Am. Chem. Soc.* **127**, 15336 (2005).
- ²¹S. M. Huang, X. Y. Cai, and J. Liu, *J. Am. Chem. Soc.* **125**, 5636 (2003).
- ²²L. X. Zheng, M. J. O'Connell, S. K. Doorn, X. Z. Liao, Y. H. Zhao, E. A. Akhadov, M. A. Hoffbauer, B. J. Roop, Q. X. Jia, R. C. Dye, D. E. Peterson, S. M. Huang, J. Liu, and Y. T. Zhu, *Nat. Mater.* **3**, 673 (2004).
- ²³L. Shi, D. Y. Li, C. H. Yu, W. Y. Jang, D. Kim, Z. Yao, P. Kim, and A. Majumdar, *J. Heat Transfer* **125**, 881 (2003).
- ²⁴See Supplemental Material at <http://link.aps.org/supplemental/10.1103/PhysRevB.87.035406> for l_k corrections.
- ²⁵C. H. Yu, L. Shi, Z. Yao, D. Y. Li, and A. Majumdar, *Nano Lett.* **5**, 1842 (2005).
- ²⁶D. Donadio and G. Galli, *Phys. Rev. Lett.* **99**, 255502 (2007).
- ²⁷Y. Y. Zhang, Y. Xiang, and C. M. Wang, *J. Appl. Phys.* **106**, 113503 (2009).
- ²⁸D. D. T. K. Kulathunga, K. K. Ang, and J. N. Reddy, *J. Phys.: Condens. Matter* **22**, 345301 (2010).
- ²⁹A. R. Ranjbartoreh and G. Wang, *Nanoscale Res. Lett.* **6**, 28 (2011).
- ³⁰L. C. Liu, M. J. Huang, R. G. Yang, M. S. Jeng, and C. C. Yang, *J. Appl. Phys.* **105**, 104313 (2009).
- ³¹J. S. Heron, C. Bera, T. Fournier, N. Mingo, and O. Bourgeois, *Phys. Rev. B* **82**, 155458 (2010).
- ³²C. Lin, H. Wang, and W. Yang, *Nanotechnology* **21**, 365708 (2010).
- ³³S. Lepri, R. Livi, and A. Politi, *Phys. Rep.* **377**, 1 (2003).